

Highly Conductive and Flexible Paper of 1D Silver-Nanowire-Doped Graphene

Jian Chen,^{†,‡} Hui Bi,[†] Shengrui Sun,[†] Yufeng Tang,[†] Wei Zhao,[†] Tianquan Lin,[†] Dongyun Wan,[†] Fuqiang Huang,^{*,†,§} Xiaodong Zhou,^{*,‡} Xiaoming Xie,[⊥] and Mianheng Jiang[⊥]

[†]CAS Key Laboratory of Materials for Energy Conversion, Shanghai Institute of Ceramics, Chinese Academy of Sciences, Shanghai 200050, People's Republic of China

[‡]College of Chemical Engineering, East China University of Science and Technology, Shanghai 200237, People's Republic of China

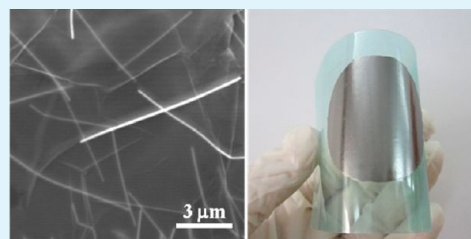
[§]College of Chemistry and Molecular Engineering, Peking University, Beijing 100871, People's Republic of China

[⊥]State Key Laboratory of Functional Materials for Informatics, Shanghai Institute of Microsystem and Information Technology, Chinese Academy of Sciences, Shanghai 200050, People's Republic of China

S Supporting Information

ABSTRACT: A novel architecture of graphene paper is proposed to consist of "1D metallic nanowires/defect-free graphene sheets". Highly conductive and flexible papers of 1D silver nanowires (Ag NWs) and chemical vapor deposition (CVD) graphene sheets as an example were fabricated by a simple filtration method. CVD graphene paper possesses much higher electrical conductivity of 1097 S/cm, compared with other reported carbon-related papers (graphene, carbon nanotube, etc.). With the addition of Ag NWs to form Ag NWs/graphene paper, the electrical conductivity is further improved up to 3189 S/cm, even higher than ~2000 S/cm of bulk graphite. Ag NWs/graphene papers have very good flexibility with the only <5% loss of electrical conductivity over 500 times mechanical bending. Highly conductive composite papers have potential in high-performance, flexible energy conversion and storage devices.

KEYWORDS: graphene, silver nanowires, flexible paper, highly electrical conductivity



Paperlike conductive materials, widely used as electrodes, have attracted more and more interest because of their potential applications in portable electronics, energy storage devices, photovoltaic cells, etc. However, it remains a major challenge to fabricate reliable materials combining electronically superior conductivity, high mechanical flexibility, and high chemical stability.

Among various materials (e.g., carbon, silver, copper, etc.), graphene has become a rising star because of its two-dimensional (2D) honeycomb structure.^{1–3} Unique properties, such as excellent electronic mobility,⁴ high specific surface area,⁵ high thermal conductivity,⁶ and high mechanical strength,^{7,8} etc., make graphene attractive. Reduced graphene oxide (RGO), chemically exfoliated from commercially available graphite, can be assembled into well-ordered and free-standing carbon-based membrane materials (hereafter referred to as graphene paper).⁹ Graphene papers are extremely superior to many other paperlike materials [carbon nanotube (CNT) or graphite paper] with mechanical strength and show potential applications in batteries, supercapacitors, and fuel cells.^{5,10–12} However, the electronic conductivity of graphene paper is as low as ~200 S/cm because of graphene domain boundaries, defects, and residual oxygen-containing groups. Although various reduction approaches were used, the electrical properties of intrinsic graphene are difficult to completely recover. Moreover, a large number of contact resistances

between small-size graphene sheets also drastically degrade the electrical transport properties. In addition, some adhesives or surfactants have been added to improve the dispersion or binding of graphene, but these can also cause an undesirable decrease in the film conductivity. These additional procedures increase the complexity of solution processing and result in high cost and low throughput. Thus, highly conductive and flexible papers with low cost and simple preparation processes are still demanded for the energy storage and photovoltaic devices.

A novel architecture of graphene papers is proposed to consist of "1D metallic nanowires/defect-free graphene sheets". Long one-dimensional (1D) metallic nanowires (silver,¹³ copper,¹⁴ CNT,¹⁵ TiN,¹⁶ etc.) play the role of framework to enhance the electrical conductivity and mechanical flexibility. In this paper, highly conductive and flexible papers of 1D silver nanowires (Ag NWs) and graphene sheets were fabricated. The paperlike material preparation involves in the simple filtration of chemical vapor deposition (CVD) graphene sheets and Ag NWs without any adhesives or surfactants. CVD graphene and Ag NWs/CVD graphene papers (hereafter referred to as graphene and Ag NWs/graphene papers, respectively) not only

Received: November 24, 2012

Accepted: January 22, 2013

Published: February 7, 2013

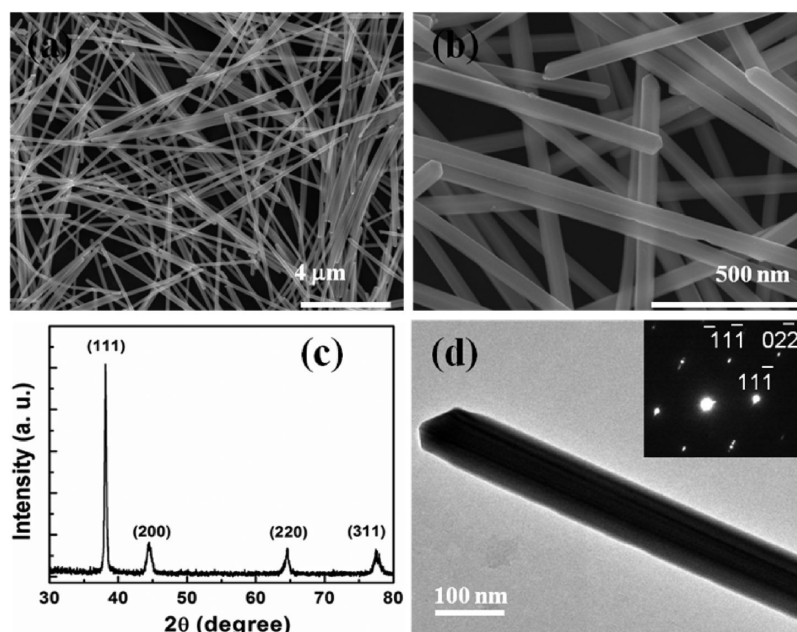


Figure 1. (a) Low- and (b) high-magnification SEM images of the as-synthesized Ag NWs by a solvothermal method. (c) XRD pattern of Ag NWs. (d) HRTEM image of an individual Ag NW with the SAED pattern in the inset.

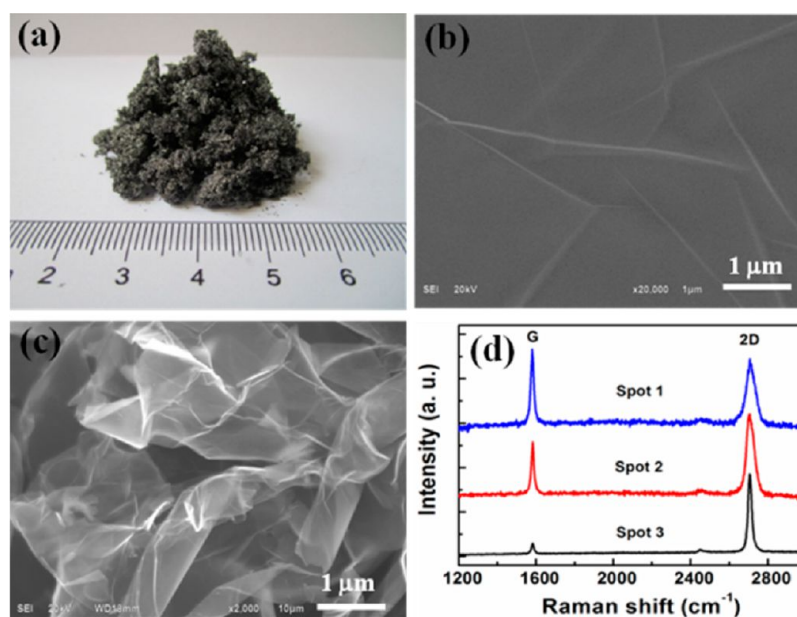


Figure 2. (a) Photograph of the CVD graphene sheets after nickel-foam etching. (b) SEM image of graphene on the substrate of nickel foam. (c) SEM image of the graphene sheets. (d) Raman spectra of graphene.

have outstanding mechanical flexibility but also exhibit extremely high electrical conductivities (up to 3189 S/cm), significantly superior to the reported graphene- and CNT-based papers.

RESULTS AND DISCUSSION

The 1D Ag NWs were synthesized at 160 °C for 2.5 h using a solvothermal method. The diameters of Ag NWs range from 150 to 200 nm, and their lengths reach up to several tens to hundreds of micrometers, as shown in Figure 1a,b. No other morphology of Ag NWs was observed, the yield of Ag NWs is almost 100% under the present synthetic conditions, and the large-scale production of Ag NWs is able to be carried out by

increasing the content of AgNO_3 or scaling up the reaction volume.

The microstructure of Ag NWs was investigated by X-ray diffraction (XRD) and high-resolution transmission electron microscopy (HRTEM). Four diffraction peaks from the XRD pattern (Figure 1c) were observed and indexed to the (111), (200), (220), and (311) planes of face-centered-cubic silver crystals. The calculated lattice constant based on the XRD pattern is 4.09 Å, close to the reported data.¹⁷ Moreover, no peaks are attributed to silver oxide to indicate the purity and high quality of Ag NWs. Furthermore, in order to obtain the detailed structural information of the Ag NW, Figure 1d shows a HRTEM image and the corresponding selected-area electron

diffraction (SAED) pattern taken from the edge of an individual Ag NW. The fringe spacings of the lattice planes are measured as 0.24 and 0.142 nm, which are consistent with separation of the Ag(111) and $-(220)$ planes. The spot feature also confirms the single-crystalline nature of Ag NWs.

3D porous structure nickel foams were used as templates for the large-scale preparation of graphene sheets by a conventional CVD method, as shown in Figure 2a. Parts b and c of Figure 2 show that graphene grew on the entire surface of nickel foam, and many suspended graphene bridging these gaps between the interfacial nickel grains were found to form continuous large-size graphene sheets. After etching of the nickel foams, the graphene sheets reveal a curved and crumpled structure with some wrinkles, and their sizes are in the range from 10 to 50 μm , much larger than graphene prepared by the Wurtz-type reductive coupling (WRC) process and RGO (their preparation procedure is described in the Supporting Information, SI).¹⁸ The quality and layer number of the graphene were further confirmed by Raman spectra,¹⁹ as shown in Figure 2d. Only G and 2D bands were observed in the absence of D bands in all of the graphene samples, suggesting a high graphene quality.²⁰ It is clear from Figure 2d that the 2D band positions are 2700, 2704, and 2706 cm^{-1} , the intensity ratios are 6.5, 1.4, and 0.8, and the full-width at half-maxima (fwhm) of the 2D band are 30, 44, and 65 cm^{-1} , respectively. These indicate that the graphene sheets are a few-layer structure, and the average layer number of graphene is 8.²¹

The graphene and Ag NWs/graphene papers were fabricated by simply filtering graphene and an Ag NWs/graphene suspension through a sheet of filter membrane, as illustrated in Figure 3a. The Ag NWs/graphene paper preparation is taken for an example. During vacuum filtration, the Ag NWs/graphene suspension penetrated throughout the filter membrane, and some small graphene sheets and Ag NWs were first

attached to the cellulose fibers by electrostatic interactions and were subsequently assembled onto the filter membrane surface. As the filtration time further increased, the cellulose surfaces and voids of the filter membrane were completely covered by graphene and Ag NWs to form a sandwich structure of Ag NWs/graphene/filter membrane (Figure 3b). The composite membrane is mechanically stable and flexible and can be shaped into desired structures and bent into large angles, as shown in Figures 3c and S1a and S1b in the SI. The free-standing graphene and Ag NWs/graphene papers can also be obtained by peeling off the filter membrane from the composite structure (Figure S1c in the SI) and easily transferred onto any desired substrates, such as conductive fluorine-doped tin oxide (FTO) and flexible and insulating polyethylene terephthalate (PET) substrates, as shown in Figure 3d,e. It is interesting to note that the Ag NWs/graphene paper on the PET was bent over 100 cycles without any damage to show its excellent flexibility.

On the basis of the above assembly procedure, a series of Ag NWs/graphene papers were prepared, and the Ag NW content varies from 0% (graphene only) to 50%. Figures 4a and S2a in the SI show typical scanning electron microscopy (SEM) images of the surface morphology of pure graphene papers. It is clear that the graphene sheets are microscale flat in the lateral dimension and only a few layers thick with some wrinkles. Figure S2b in the SI also shows the cross-sectional SEM image of the original graphene paper. The oriented layered structure was observed from the fracture edge of the original graphene papers. In contrast, for the Ag NWs/graphene papers, the graphene sheets still maintained a flat morphology, while randomly crumpled Ag NWs (tens of micrometers in length) were dispersed between graphene sheets (Figures 4b and S3a in the SI). At the same time, the Ag NWs appear to fill the pores and bridge the grain boundary between graphene sheets before starting to dominate the papers, as shown in Figure S3b,c in the SI. The inserted Ag NWs can not only effectively prevent self-stacking of graphene sheets after filtration but also act as a conductive bridge between the graphene sheets to provide effective electron-transport channels.²²

Electrical measurements of graphene and Ag NWs/graphene papers with a thickness of about 25 μm were conducted using the four-probe technique with silver electrodes. The electrical conductivity as a function of the Ag NW content is plotted in Figure 4c. It clearly reveals that the pure graphene papers show extremely outstanding electrical properties, and the electrical conductivity reaches up to 1097 S/cm, much higher than those of graphite flake (291 S/cm), WRC graphene (3.0 S/cm), and RGO (1.2 S/cm) assembled papers prepared from the same procedure. The specific electrical conductivities are listed in Figure 4d and Table 1.

Such high electrical conductivity of the graphene paper is mainly attributed to the high quality of graphene and the preparation procedure. First, the graphene sheets directed by a 3D nickel foam template have high crystalline and perfect crystal structure, which greatly reduces the possibility of scattering electrons inside graphene. Moreover, although graphite flakes have nearly the same crystalline quality, the graphene sheets are much larger than the graphite flakes in size, as shown in Figure S4 in the SI. Thus, the large-size graphene sheets assembled into graphene papers also significantly eliminate the contact resistance between graphene sheets. Furthermore, the simple fabrication process forms self-assembling order graphene papers without needing any extra adhesives or surfactants. Therefore, the electrical properties of

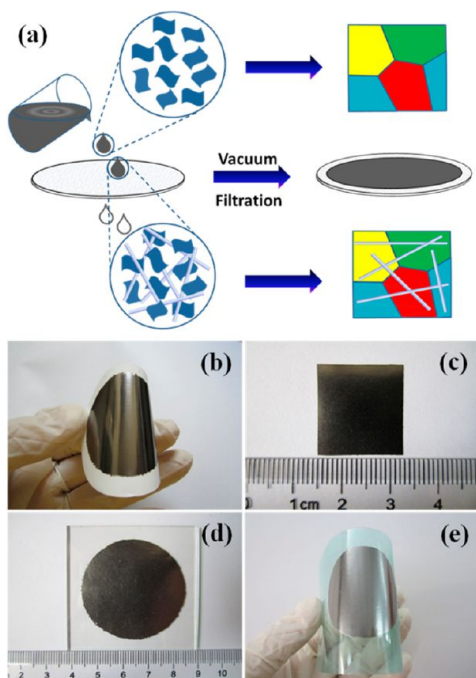


Figure 3. (a) Schematic fabrication procedure of the Ag NWs/graphene papers and photographs of (b) Ag NWs/graphene/filter membrane, (b) free-standing Ag NWs/graphene paper, and Ag NWs/graphene papers on (d) FTO and (e) PET substrates, respectively.

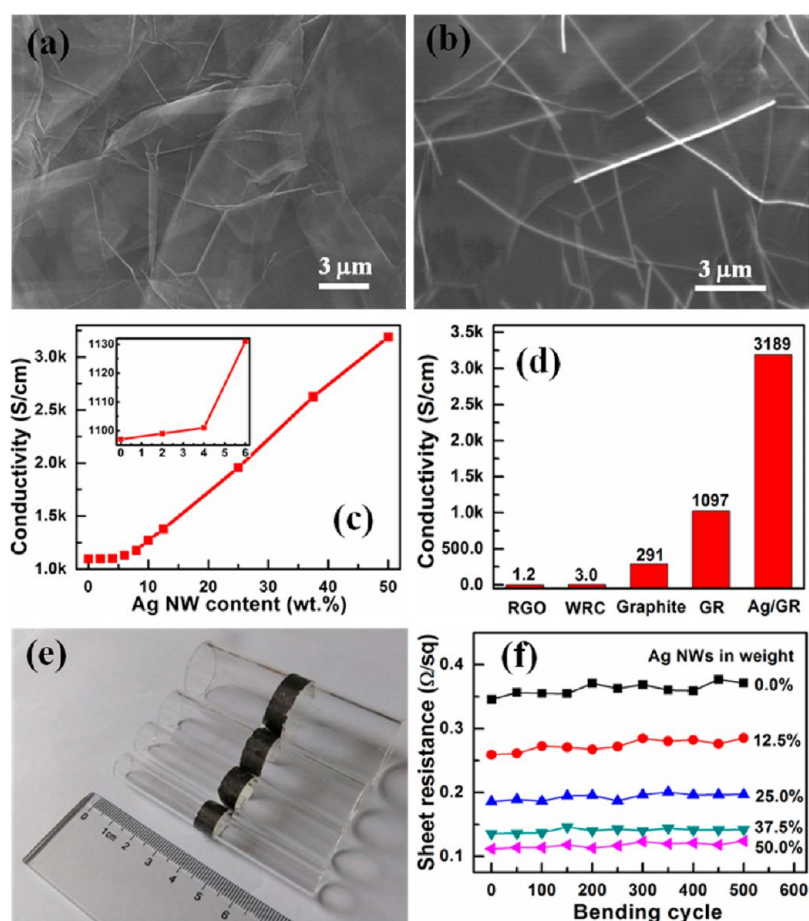


Figure 4. SEM images of (a) graphene and (b) Ag NWs/graphene papers. (c) Electrical conductivities of Ag NWs/graphene papers. Inset: electrical conductivities of Ag NWs/graphene papers with the low concentrations of Ag NWs. (d) Comparison of the electrical conductivities of the RGO, WRC graphene, graphite, graphene, and Ag NWs/graphene papers. (e) Photograph of the Ag NWs/graphene papers to reveal their flexibility. (f) Sheet resistance deviations of the different Ag NWs/graphene papers in the bending tests at a constant radius of curvature of 5 mm.

Table 1. Sheet Resistance (R_s) and Electrical Conductivity (σ) Comparisons of the Ag NWs/Graphene Papers

sample	R_s (Ω/sq)	σ (S/cm)	reference
RGO	400	1.2	this work
WRC graphene	118	3.0	this work
graphite flakes	3.01	291	this work
CVD graphene	0.33	1097	this work
2.0 wt % Ag NWs/CVD graphene	0.33	1099	this work
4.0 wt % Ag NWs/CVD graphene	0.32	1101	this work
6.0 wt % Ag NWs/CVD graphene	0.31	1131	this work
8.0 wt % Ag NWs/CVD graphene	0.30	1177	this work
10.0 wt % Ag NWs/CVD graphene	0.28	1272	this work
12.5 wt % Ag NWs/CVD graphene	0.26	1378	this work
25 wt % Ag NWs/CVD graphene	0.18	1957	this work
37.5 wt % Ag NWs/CVD graphene	0.14	2626	this work
50 wt % Ag NWs/CVD graphene	0.11	3189	this work
highly RGO		72–160	23
$\text{RGO}_{\text{HI-AcOH}}$		304	25

graphene papers are significantly superior to those of papers assembled from graphene, CNT, activated carbon, graphite, and other carbon-based materials reported previously.^{9,23–25}

In order to further improve the electrical properties of graphene papers, Ag NWs were used as 1D conductive agents to assemble into Ag NWs/graphene papers, and the corresponding electrical conductivities are shown in Figure

4c. At the low concentrations (~ 4.0 wt %) of Ag NWs, the Ag NWs/graphene papers show almost the same conductivity as the pure graphene paper. When the content of Ag NWs further increases to 6.0%, the electrical conductivity rapidly increases up to 1131 S/cm, as shown in the inset of Figure 4c. After 8%, 10%, 12.5%, 25%, 37.5%, and 50% Ag NWs are added, the electrical conductivities of the CVD Ag NWs/graphene papers reach up to 1176, 1271, 1378, 1957, 2626, and 3189 S/cm, respectively, showing an almost 3-fold increase with respect to the pure CVD graphene paper. The value is far larger than that of bulk graphite (2.0×10^3 S/cm). The conductive behavior is similar to the reported results.²⁶ These data demonstrate that the Ag NWs have an enhanced effect on the electrical properties of the graphene papers, which is mainly due to the very highly conductive Ag NW bridges between graphene sheets to form a continuous conducting network, as shown Figures 4b and S3 in the SI. Therefore, it is reasonably considered that the Ag NWs/graphene papers will be tailored to satisfy the requirements of practice applications.

The free-standing and highly conductive papers possess excellent mechanical flexibility, as shown in Figure 4e,f. In order to evaluate the mechanical stability performance of Ag NWs/graphene, bend cycles using a radius of curvature of 5 mm were conducted for Ag NWs/graphene papers with different Ag NW contents (~ 50 wt %). The conductive paper was bent over 500 times to result in better mechanical flexibility, and their

resistance deviations are less than 5%. The outstanding mechanical flexibility is likely due to the combined effect of the intrinsic flexibility of an individual Ag NW and graphene and the strong binding between the graphene and Ag NWs. The flexibility and free-standing properties of the composite papers provide them with potential applications in flexible electronics, energy storage, photovoltaic devices, etc.

CONCLUSION

The architecture of the graphene papers, "1D metallic nanowires/defect-free graphene sheets", consists of 1D Ag NWs and CVD graphene sheets as an example. The large-scale preparation of high-quality graphene and Ag NWs was performed by the CVD method and a solvothermal process. The as-prepared free-standing graphene and Ag NWs/graphene papers have excellent electrical conductivity and good flexibility, superior to those of the other reported graphene, CNT-based papers. Because of excellent electrical conductivity, high thermal and chemical stability, and desirable flexibility, the graphene and Ag NWs/graphene papers may find applications in high-performance, flexible energy conversion and storage devices.

EXPERIMENTAL SECTION

Graphene Preparation. High-quality graphene sheets were deposited by the CVD method on fresh nickel foams in a quartz tube, and a mixture gas of 300 sccm Ar and 50 sccm H₂ was introduced to remove the residual air for 30 min. The quartz tube was heated rapidly to 1000 °C and annealed for 10 min under the H₂ and Ar gas flow. Then, a 10 sccm CH₄ flow was introduced to grow graphene on the nickel foam surface for 10 min, and the sample was subsequently cooled rapidly to room temperature. Finally, the sample was immersed in a 5 M HCl solution for completely etching the nickel foam, and the CVD graphene was obtained by filtering the solution and drying in a vacuum oven at 70 °C for 12 h.

Ag NW Preparation. Ag NWs were prepared using a solvothermal method. Briefly, a 10 mL ethylene glycol (EG) solution of 0.1 mM FeCl₃ was vigorously stirred after the addition of 0.15 M poly(vinylpyrrolidone). The mixed solution was injected drop by drop using a syringe into 10 mL of a magnetically stirred EG solution of AgNO₃ (0.1 M). Then, the solution was placed in a 25 mL Teflon-lined autoclave tube. The tube was sealed and heated at 160 °C for 2.5 h and then cooled naturally to room temperature. Ag NWs were collected by the addition of a large amount of acetone, followed by sonication and centrifugation.

Ag NWs/Graphene Paper Fabrication. CVD graphene and Ag NWs were dispersed in deionized water, and the concentration was about 0.2 mg/mL. After bath sonication for 5 min, the Ag NWs/graphene suspension was further probe-sonicated at a power of 200 W for 30 min and filtered to form Ag NWs/graphene/filter membrane. The thickness of Ag NWs/graphene was controlled by adjusting the volume and/or concentration of the Ag NWs/graphene suspension. The Ag NWs/graphene membrane was peeled off from the filter to obtain free-standing papers, which can be transferred onto a desired substrate (e.g., PET, glass, quartz, FTO, etc.).

Characterization and Measurement. The morphologies and structures of the graphene papers were investigated by SEM (JEOL JSM-6510 and Hitachi S-4800), XRD (Bruker D8 Advance), HRTEM (JEOL JEM 2100F), and SAED. Raman spectra of graphene were obtained with Raman spectroscopy with a laser excitation energy of 532 nm. The electrical properties of graphene papers were measured by the Van der Pauw method with an Accent HL5500.

ASSOCIATED CONTENT

Supporting Information

Preparation procedure of WRC graphene and RGO, optical photographs, and SEM images of graphene, Ag NWs/graphene, and graphite. This material is available free of charge via the Internet at <http://pubs.acs.org>.

AUTHOR INFORMATION

Corresponding Author

*Tel.: +86-21-52411660 xdzhou@ecust.edu.cn (F.Q.H.). Fax: +86-21-52416360 (F.Q.H.). E-mail: huangfq@mail.sic.ac.cn (F.Q.H.), (X.Z.).

Author Contributions

Dr. Jian Chen and Hui Bi equally contributed to this work.

Notes

The authors declare no competing financial interest.

ACKNOWLEDGMENTS

Financial support from 863 Program of China (Grant 2011AA050505), the NSF of China (Grants 11274328, 51202274, 51202275, 91122034, 51125006, 51121064), the STC of Shanghai (Grant 12JC1409000), the CAS/SAFEA International Partnership Program for Creative Research Teams, and Chinese Academy of Sciences (Grants KJCX2-EW-W11, KGZD-EW-303) are acknowledged.

REFERENCES

- (1) Novoselov, K. S.; Geim, A. K.; Morozov, S. V.; Jiang, D.; Zhang, Y.; Dubonos, S. V.; Grigorieva, I. V.; Firsov, A. A. *Science* **2004**, *306*, 666–669.
- (2) Huang, X.; Zeng, Z.; Fan, Z.; Liu, J.; Zhang, H. *Adv. Mater.* **2012**, *24*, 5979–6004.
- (3) Huang, X.; Yin, Z.; Wu, S.; Qi, X.; He, Q.; Zhang, Q.; Yan, Q.; Boey, F.; Zhang, H. *Small* **2011**, *7*, 1876–1902.
- (4) He, Q.; Wu, S.; Yin, Z.; Zhang, H. *Chem. Sci.* **2012**, *3*, 1764–1772.
- (5) Zhu, Y.; Murali, S.; Stoller, M. D.; Ganesh, K. J.; Cai, W.; Ferreira, P. J.; Pirkle, A.; Wallace, R. M.; Cychosz, K. A.; Thommes, M.; Su, D.; Stach, E. A.; Ruoff, R. S. *Science* **2011**, *332*, 1537–1541.
- (6) Chen, S.; Wu, Q.; Mishra, C.; Kang, J.; Zhang, H.; Cho, K.; Cai, W.; Balandin, A. A.; Ruoff, R. S. *Nat. Mater.* **2012**, *11*, 203–207.
- (7) Lee, C.; Wei, X.; Kysar, J. W.; Hone, J. *Science* **2008**, *321*, 385–388.
- (8) Huang, X.; Qi, X.; Boey, F.; Zhang, H. *Chem. Soc. Rev.* **2012**, *41*, 666–686.
- (9) Dikin, D. A.; Stankovich, S.; Zimney, E. J.; Piner, R. D.; Dommett, G. H. B.; Evmenenko, G.; Nguyen, S. T.; Ruoff, R. S. *Nature* **2007**, *448*, 457–460.
- (10) El-Kady, M. F.; Strong, V.; Dubin, S.; Kaner, R. B. *Science* **2012**, *335*, 1326–1330.
- (11) Li, S.; Luo, Y.; Lv, W.; Yu, W.; Wu, S.; Hou, P.; Yang, Q.; Meng, Q.; Liu, C.; Cheng, H. M. *Adv. Energy Mater.* **2011**, *1*, 486–490.
- (12) Hu, L.; Choi, J. W.; Yang, Y.; Jeong, S.; La Mantia, F.; Cui, L. F.; Cui, Y. *Proc. Natl. Acad. Sci. U.S.A.* **2009**, *106*, 21490–21494.
- (13) De, S.; Higgins, T. M.; Lyons, P. E.; Doherty, E. M.; Nirmalraj, P. N.; Blau, W. J.; Boland, J. J.; Coleman, J. N. *ACS Nano* **2009**, *3*, 1767–1774.
- (14) Liang, J.; Bi, H.; Wan, D. Y.; Huang, F. Q. *Adv. Funct. Mater.* **2012**, *22*, 1267–1271.
- (15) Hu, L.; Hecht, D. S.; Gruner, G. *Nano Lett.* **2004**, *4*, 2513–2517.
- (16) Dong, S.; Chen, X.; Gu, L.; Zhou, X. H.; Li, L. F.; Liu, Z. H.; Han, P. X.; Xu, H. X.; Yao, J. H.; Wang, H. B.; Zhang, X. Y.; Shang, C. Q.; Cui, G. L.; Chen, L. Q. *Energy Environ. Sci.* **2011**, *4*, 3502–3508.
- (17) Sun, Y.; Xia, Y. *Adv. Mater.* **2002**, *14*, 833–837.

- (18) Lin, T. Q.; Huang, F. Q.; Liang, J.; Wang, Y. *Energy Environ. Sci.* **2011**, *4*, 862–865.
- (19) Ferrari, A. C.; Meyer, J. C.; Scardaci, V.; Casiraghi, C.; Lazzeri, M.; Mauri, F.; Piscanec, S.; Jiang, D.; Novoselov, K. S.; Roth, S.; Geim, A. K. *Phys. Rev. Lett.* **2006**, *97*, 187401–187404.
- (20) Chen, Z.; Ren, W.; Gao, L.; Liu, B.; Pei, S.; Cheng, H. M. *Nat. Mater.* **2011**, *10*, 424–428.
- (21) Bi, H.; Huang, F. Q.; Liang, J.; Tang, Y. F.; Lv, X. J.; Xie, X. M.; Jiang, M. H. *J. Mater. Chem.* **2011**, *21*, 17366–17370.
- (22) Jeong, C.; Nair, P.; Khan, M.; Lundstrom, M.; Alam, M. A. *Nano Lett.* **2011**, *11*, 5020–5025.
- (23) Park, S.; An, J.; Jung, I.; Piner, R. D.; An, S. J.; Li, X.; Velamakanni, A.; Ruoff, R. S. *Nano Lett.* **2009**, *9*, 1593–1597.
- (24) Li, D.; Muller, M. B.; Gilje, S.; Kaner, R. B.; Wallace, G. G. *Nat. Nanotechnol.* **2008**, *3*, 101–105.
- (25) Moon, I. K.; Lee, J.; Ruoff, R. S.; Lee, H. *Nat. Commun.* **2010**, *1*, 73–79.
- (26) Chun, K. Y.; Oh, Y.; Rho, J.; Ahn, J. H.; Kim, Y. J.; Choi, H. R.; Baik, S. *Nat. Nanotechnol.* **2010**, *5*, 853–857.